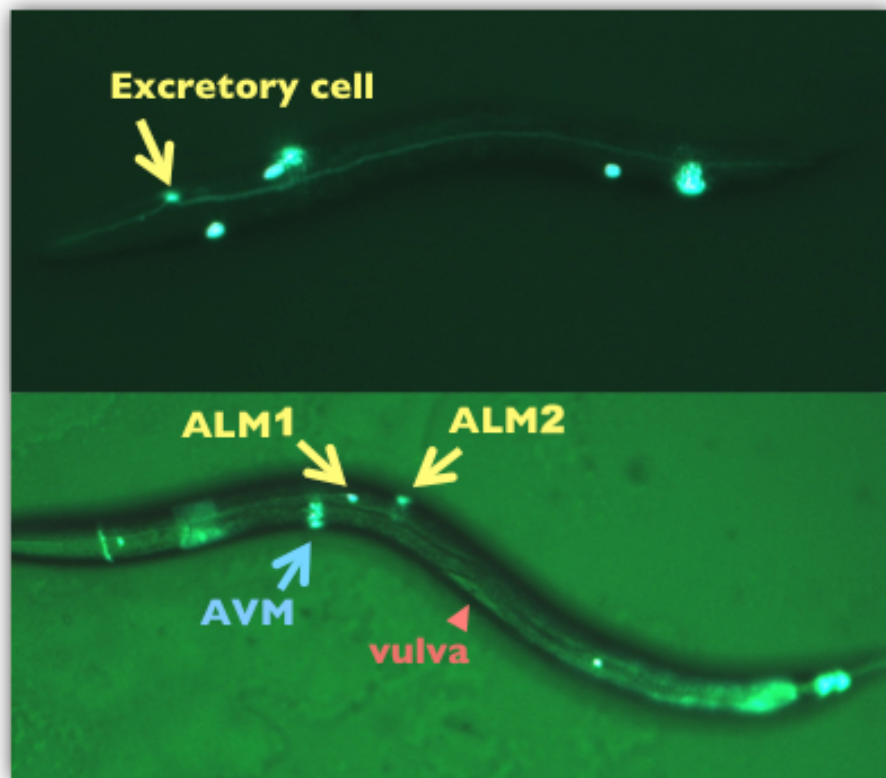


FUNCTIONAL ANALYSIS OF MIG-10:

a cytoplasmic adaptor protein important in neuronal migration and process out-growth in *C. elegans*



BY:
Subaiou Zhang

FUNCTIONAL ANALYSIS OF MIG-10:

a cytoplasmic adaptor protein important in neuronal migration and process out-growth in *C. elegans*

An Major Qualifying Project
submitted to the Faculty of
WORCESTER POLYTECHNIC INSTITUTE
in partial fulfillment of the requirements for the
degree of Bachelor of Science

by
Subaiou Zhang

Date:
Apr 25, 2010

Report Submitted to:

Professor Elizabeth Ryder
Worcester Polytechnic Institute

This report represents work of WPI undergraduate students submitted to the faculty as evidence of a degree requirement. WPI routinely publishes these reports on its web site without editorial or peer review. For more information about the projects program at WPI, see <http://www.wpi.edu/Academics/Projects>.

TABLE OF CONTENTS

Abstract	1
Acknowledgments	2
Introduction	3
Background	4
<i>Terms & Abbreviations</i>	4
<i>C. elegans as genetic model system</i>	5
<i>Axon guidance</i>	5
<i>MIG-10: cytoplasmic signaling protein, ortholog of Lamellipodin</i>	7
<i>Function of MIG-10 and a proposed model of the mechanism</i>	9
<i>ABI-1</i>	11
Project Goal A: Test whether different isoforms of MIG-10 rescue different aspects of mig-10 mutant phenotype	12
Project Goal B: Preparation of Co-immunoprecipitation to test MIG-10/ ABI-1 interaction in insect system	12
Materials & Methods	13
Transformation of competent cells	13
Isolation of plasmid DNA	13
Gel Electrophoresis	14

Sequencing	14
Maintaining Strains	14
Preparation of worms slides for quantification	16
Quantification of Phenotypes	17
Statistical Analysis	17
Results	18
Genetic crosses	18
FosAB rescues mig-10 mutant excretory canal truncation	21
FosAB rescues mig-10 mutant ALM & AVM cell migration	22
Cell-autonomous expression of MIG-10A rescues ALM but not AVM cell migration	24
Preparation of Co-IP	26
Discussion	29
References	31

Abstract

The *C. elegans* protein MIG-10 is known to facilitate the connections between surface guidance signals with cellular responses during neuronal migration. Mutations in *mig-10* result in defects in axon guidance, neuronal migration, and excretory canal outgrowth. Strains were constructed using GFP markers and *mig-10* genomic constructs and were used to determine which MIG-10 isoforms are necessary to rescue *mig-10* defects. Quantitative results indicate that either MIG-10A or B or both isoforms are sufficient to rescue defects in both excretory canal and cell migration. Cell-autonomous expression of MIG-10A can rescue migration of ALM neurons.

Acknowledgments

I would like to thank the Colón-Ramos lab, as the fosmids strains used in this project were kindly made available to us by Dr. Daniel Colón-Ramos.

I would like to thank Professor Sam Politz for his kind support and for letting me use his compound microscope. I would like to thank my lab-mate Molly McShea, whose presence constantly beautified our lab, for the help and company she offered me, and for being a role model as a fine graduate student. I would like to thank the good people of the Gateway Shuttle, without whom I would have likely done no work during the winter.

I could not give enough thanks to my advisor, Elizabeth Ryder, for the generous guidance, patience, and much greater understanding of statistical analysis she has given me. Perhaps much more important than the research skills I have gained during my work, I have truly enjoyed working with her and have learned so much from her on both professional and personal levels. Her mentorship has laid the foundation upon which my future scientific endeavors will stand.

Introduction

The study of developmental neurobiology aims to understand the cellular and molecular mechanisms underlying formation of nervous systems during embryonic development and throughout life (Yaron & Zheng, 2007). The intricate network of connections between neurons is essential for the information-processing performance of our nervous system (Tessier-Lavigne & Goodman, 1996). In a developing central nervous system, neurons must find their paths and navigate to their correct targets over great distances (Patel & Van Vactor, 2002) to make proper connections in order to form the correctly wired network of neural circuits (Quinn & Wadsworth, 2008). Neurons accomplish this by detecting and responding to extracellular guidance cues, which guide axons along specific pathways to travel to their appropriate destinations (Dickson, 2002; Tessier-Lavigne & Goodman, 1996). It is important to understand how neural connectivity is established because mis-wiring of neural circuits can lead to a dysfunctional nervous system associated with developmental disorders including autism and Down's syndrome (Quinn & Wadsworth, 2008). The knowledge of guidance mechanisms will also shed light on the recovery of adult nervous system after injury (Yaron & Zheng, 2007) and neurodegenerative diseases such as Alzheimer's disease (Quinn & Wadsworth, 2008).

Extensive studies on neuronal and axonal migration have led to much progress on the molecular identification of these guidance molecules and their surface receptors (Dickson, 2002; O'Donnell et al., 2009; Yaron & Zheng, 2007). However, the cytoplasmic signaling mechanisms underlying the coordination and integration of guidance activities are still being explored (Dickson, 2002; Yu & Bargmann, 2001). Naturally, to study the genes and their translated proteins involved in axon guidance is essential to complete our understanding of the developing nervous system. *C. elegans* protein MIG-10, which facilitates the connections

between surface guidance signals with cellular responses, is studied for its role in signal transduction pathways. In this project, different isoforms of MIG-10 were tested to determine if they are necessary to rescue different aspects of MIG-10 phenotype. Quantitative results indicate that either MIG-10A or B or both isoforms are sufficient to rescue *mig-10* defects in both excretory canal truncation and cell migration. MIG-10A was also expressed cell-autonomously and showed rescue of ALM but not AVM neuron migration. Another goal of this project was to initiate the preparation for testing the interactions between MIG-10 and ABI-1 by co-immunoprecipitation in an insect system to confirm their interactions identified previously in a yeast two hybrid screen (Gossellin & O'Toole, 2008). Expression vectors were generated using the Gateway System© from Invitrogen.

BACKGROUND

Terms & Abbreviations

ABI	Abl-Interacting
ALM	Anterior Lateral Microtubule neuron
AVM	Anterior Ventral Microtubule neuron
CANs	Canal Associated Neurons
DCC	Deleted in Colorectal Cancer
Ena/VASP	Enabled/VASodilator-Stimulated Phosphoprotein
HSNs	Hermaphrodite-Specific Neurons
MIG	abnormal cell MIGration
PH	Pleckstrin Homology
RA	Ras Association
RIAM	Rap-1 InterActing Molecule
Robo	roundabout
SLT	Slit
UNC	UNCoordinated

C. elegans as genetic model system

The small, translucent, free-living nematode *Caenorhabditis elegans* (*C. elegans*) was the first multicellular organism with its complete genome sequenced (Hodgkin, 2005), and has since become a powerful model system for genetic analysis which can be easily manipulated genetically owing to its small size and rapid life cycle (Manser et al., 1997; Manser & Wood, 1990). *C. elegans*'s nervous system, the nematode's most complex organ with the most cells (302 neurons) and the largest cellular diversity, has been characterized extensively (Hobert, 2005). Especially suited for cell migration analysis, all cell movements and divisions in wild-type *C. elegans* development have been characterized with consistency among individuals (Manser et al., 1997). The ability to test the interactions of phenotypically similar mutant genes *in vivo* is another important feature of *C. elegans*, one utilized in many related studies including this project dealing with complex and overlapping signaling pathways.

Axon guidance

Axon guidance refers to the stage in a developing nervous system during which axons are guided in response to various extracellular guidance cues to reach their appropriate targets (Yoshikawa & Thomas, 2004) and eventually to establish the correct neural network connections (Quinn & Wadsworth, 2008). The precisely coordinated guidance and growth process of axons are led by the growth cones, which are specialized, dynamic and sensory-motile fan-shaped structures at the distal tips of developing axons (Dickson, 2002; Drees & Gertler, 2008; Quinn & Wadsworth, 2008). Specific receptors on the growth cones recognize and respond to a variety of attractive or repulsive, short-range and long-range guidance cues in the extracellular environment (Dickson, 2002; Yoshikawa & Thomas, 2004) by rear-

ranging cytoskeleton and altering the direction of outgrowth (Lundquist *et al.*, 2001). Specifically, local accumulation of F-actin and microtubules occurs in the growth cones, which subsequently migrate in the direction of accumulation (Quinn, 2008). In a typical growth cone, finger-like protrusions called filopodia built from parallel F-actin bundles extend beyond the lamellipodium, a dense two-dimensional actin web (Chang *et al.*, 2006; Drees & Gertler, 2008).

By the early 1990s, genetic, biochemical and molecular approaches had led to the discovery of four well-characterized families of instructive extracellular guidance cues, including the netrins, Slits, semaphorins, and ephrins (Dickson, 2002; Yu & Bargmann, 2001). These cues function by either attracting (stimulating outgrowth) or repelling (inhibiting outgrowth) axons through activating the surface receptors on the migrating growth cones (Quinn, 2008). The transmembrane receptors for each of these cues have also been identified. In the cases of netrins (UNC-40/DCC and UNC-5 receptors) and Slits (Robo receptors), only a few ligands and receptors interact with each other, while semaphorins (neuropilin and plexin receptors) and ephrins (Eph receptors) have large families of related ligands to interact with receptor protein families (Yu & Bargmann, 2001). In addition, recent studies have revealed that typical morphogens, known best for their effects on early embryonic patterning (Chilton, 2006), can also function as axon guidance molecules (Yoshikawa & Thomas, 2004). The Wingless-type (Wnt) proteins, Sonic hedgehog (Shh), TGF- β and FGFs are such secreted patterning molecules and have been identified as axon guidance molecules in various species (Killeen & Sybingco, 2008). Interestingly, the number of guidance cues and receptors seem small relative to the vast number of axons they direct to make the intricate connections which form complex neural networks (Chilton, 2006; Dickson, 2002; Yu & Bargmann, 2001). As described before, much progress has been made in the charac-

terization of molecular cues, receptors and their ligands, yet the understanding of the cytoplasmic signaling mechanisms that enable cells to respond to guidance cues and to transmit the signals into changes in growth cone motility remain incomplete (Patel & Van Vactor, 2002).

MIG-10: cytoplasmic signaling protein, ortholog of Lamellipodin

The *C.elegans* protein MIG-10 belongs to the MRL family of cytoplasmic adaptor proteins, which include MIG-10, the vertebrate proteins RIAM and Lamellipodin. The members of MRL protein family share conserved Ras association (RA) and pleckstrin homology (PH) domains, and a proline-rich regions found commonly in signal transduction pathways (Lafuente et al., 2004). Found downstream of cell surface molecules, the MRL adaptor proteins are shown to be involved in receptor activation and cellular response in axon guidance and migration (Krause et al., 2004).

The *mig-10* gene was discovered in a screen for defective neuronal migration in *C. elegans*. Mutations in the *mig-10* gene cause defects in neuronal migration, axon guidance and the outgrowth of the excretory canal cell (Manser & Wood, 1990). A premature stop codon in the *mig-10* (*ct41*) mutant allele results in mutant animals with incomplete migration of three migratory neurons CAN, ALM and HSN despite the fact that CAN and ALM migrate from anterior to posterior while HSN migrates from posterior towards anterior, indicating that the *mig-10* mutation defect lies in the migration mechanism (Manser & Wood, 1990). Defects in axon guidance are also found in *mig-10* mutants, such as irregular ventral and lateral neuronal branching in HSN and loss of axonal branching in AVM (Chang et al., 2006). In addition, the *mig-10* mutation leads to the truncated outgrowth of the excretory canal, which bears similarities with axon outgrowth (Hedgecock et al., 1987) and has exhib-

ited the same truncated phenotype in animals that have mutations in other genes that affect axon guidance. Interestingly, genetic mosaic analysis suggests that MIG-10 functions cell non-autonomously in development of the excretory canal, meaning that MIG-10 might not function in the excretory canal itself but in the epidermal cells surrounding the excretory canal (Manser *et al.*, 1997). All the mutant defects described above can be identified and quantified in live worms by analyzing transgenic markers of particular subsets of neurons or the outgrowth of the excretory canal.

Conserved with its vertebrate homologs RIAM and Lpd, MIG-10 contains a Ras-Interacting (RA) domain, a lipid-binding Pleckstrin Homology (PH) domain and a proline-rich region (Figure 1). The RA domain has been shown to interact with the GTPase CED-10/Rac (Quinn *et al.*, 2008). The PH domain of Lpd binds to the membrane phospholipid PI(3,4)P2 (phosphotydyl inositol bisphosphate), a product of the vertebrate homologue to AGE-1 (Krause *et al.*, 2004). The MRL family of proteins are known to interact with members of the Ena/VASP family of proteins which are involved in actin polymerization, most likely through the binding of the proline rich region to the EVH1 region of the Ena/VASP proteins. (Krause *et al.*, 2004; Quinn *et al.*, 2006).

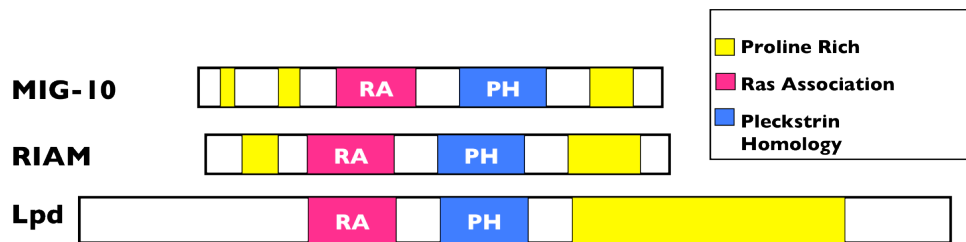


Figure 1. Domain structure of the MRL proteins (Ficociello and Ryder, unpublished data).

Currently, three transcripts of MIG-10 isoforms have been identified (Figure 2). Two isoforms MIG-10A and MIG-10B, which contain domains similar to mammalian G-proteins, were identified by Manser *et al.* in 1977. The third isoform transcript *mig-10c* has been dis-

covered later (Manser et al., 1997). The three transcripts are expressed from different promoter regions and exhibit differences in their initial exons (Quinn et al., 2006). The three protein isoforms differ in their N-terminal regions, with MIG-10A and MIG-10C containing additional proline rich regions when compared with the shortest isoform MIG-10B.

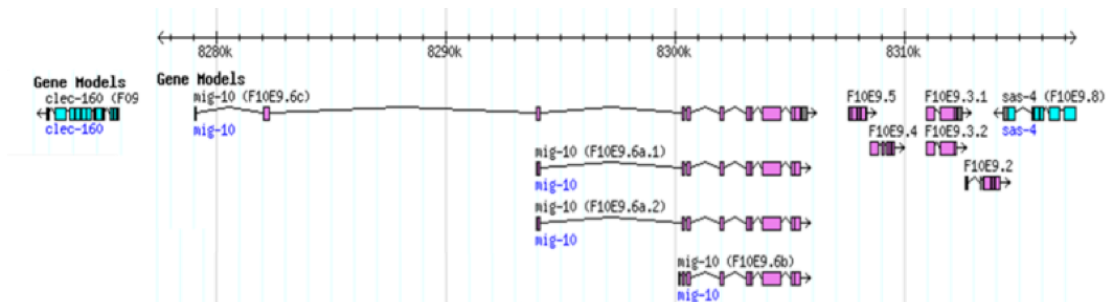


Figure 2. mig-10 transcripts.

The three mig-10 transcripts (A, B, and C) are shown at the top of the figure. Purple boxes represent exons. Transcript mig-10a.2 is identical to mig-10a.1, except that the noncoding region is 2 bps longer. Taken from Wormbase (<http://www.wormbase.org/>).

Function of MIG-10 and a proposed model of the mechanism

During axon guidance, MIG-10 has been shown to function downstream of the guidance cues UNC-6/netrin (and its receptor UNC-40/DCC) and SLT-1/Slit and its receptor Robo (Chang et al, 2006; Quinn, et al., 2006; Quinn, et al., 2008). Overexpression of MIG-10 in the absence of UNC-6 and SLT-1 causes multiple undirected processes to form, indicating MIG-10's outgrowth-promoting function. This outgrowth-promoting activity can be polarized and oriented by the addition of either guidance cue and leads to the formation of a single process with enhanced guidance (Quinn, et al., 2006). Investigations of the signaling pathway have also found that MIG-10 interacts with other proteins involved in actin polymerization. For example, MIG-10 was found to work in conjunction with UNC-34/Ena, yet both also have distinct functions. This was suggested by the fact that the mig-10;unc-34

double mutant results in more severe axon guidance defects than either single mutant alone. (Chang et. al, 2006). In this same study the interaction of MIG-10 and phosphoinositide-3 kinase (PI3K) AGE-1 was also examined. AGE-1 is a regulator of MIG-10 in the guided axon growth for AVM. Over expression of MIG-10 resulted in excessive growth of axons whereas a null mutation of AGE-1 suppressed the excessive outgrowth, indicating that AGE-1 acts upstream of MIG-10 in the development of axons.

A proposed model for the possible sequence of events of the mechanism is demonstrated in Figure 3. Extracellular guidance cue activates UNC-40/DCC receptor, which in turn activates a PI3K and the CED-10/Rac GTPase. This PI3 kinase is most likely AGE-1, suggested based on the evidence that a null mutation of AGE-1 suppresses the excessive outgrowth of axons caused by over expression of MIG-10 (Chang et al., 2006). After localizing to the vicinity of cell membrane, MIG-10 protein associates with the Ras-related protein and PI(3,4)P₂ phospholipids produced by the PI3 kinase via its RA domain and its PH domain respectively. The Ena/VASP protein UNC-34 is then localized through binding to MIG-10 and actin polymerization subsequently occurs in response to the activation of UNC-34 (Quinn et al, 2006).

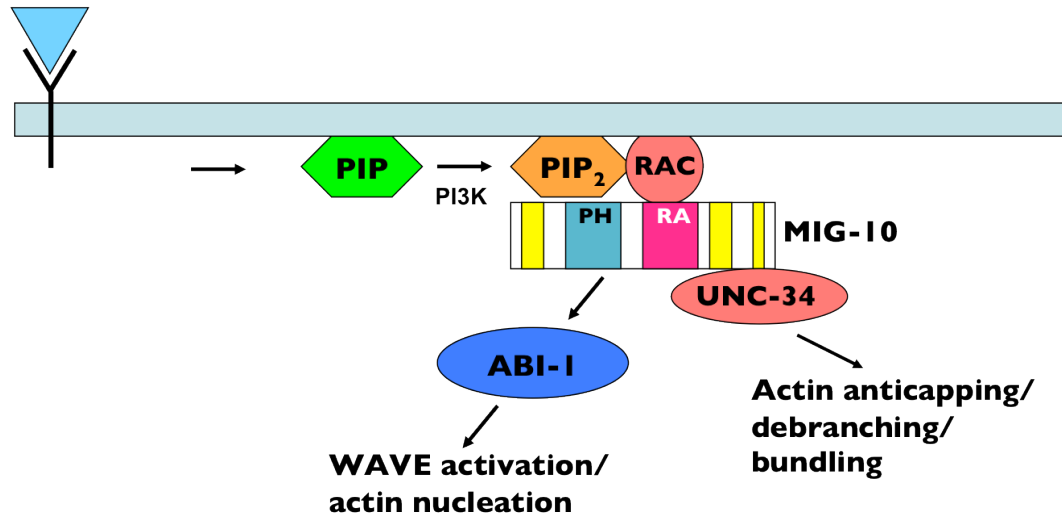


Figure 3. Speculative Model for MIG-10 function. (Ficociello and Ryder, 2007).

In response to a guidance cue, CED-10/Rac GTPase and PI3 kinase are activated, resulting in localization of MIG-10 and associated proteins related to actin polymerization to this region of the membrane.

ABI-1

ABI-1 was previously identified to be interacting with MIG-10 in a yeast two hybrid screen (Gossellin and O'Toole, 2008). Abelson interacting protein-1 (ABI-1) is a component of the WAVE complex, essential for the formation and activation of the WAVE2 signaling complex. WAVE2 actively binds Rac-GTP, which relieves the inhibition of WAVE1, allowing the WAVE/SCAR complex to mediate actin filament nucleation and participate in actin remodeling by activating the Arp2/3 complex (Innocenti et al, 2004). The interaction between ABI-1 and MIG-10 supports the proposed model of MIG-10 function with actin polymerizing proteins recruited in axon guidance by guidance cues. In addition to its role in actin polymerization and dendrite branching, ABI-1 protein is implicated in phosphorylation and localization of protein complexes to cellular sub-compartments as well as in actin reorganization (Proepper, et al., 2007). Loss of ABI-1 function results in both axon guidance defects and truncation of the excretory canal. It is suggested that ABI-1 acts cell autonomously in both neurons and the excretory cell (Schmidt et al., 2009).

PROJECT GOAL A: Test whether different isoforms of MIG-10 rescue different aspects of *mig-10* mutant phenotype

The main goal of this Major Qualifying Project (MQP) was to determine which MIG-10 isoforms are necessary for MIG-10 function in neuronal migration and excretory canal outgrowth. It has been hypothesized that different MIG-10 isoforms function in migrating neurons and underlying epidermal cells along which migrations occur. Genomic constructs including different combinations of MIG-10 isoforms were used to create transgenic mutant *C.elegans* strains labeled with markers of the excretory canal (*pgp-12::GFP*) or migratory neurons ALM and AVM (*flp-20::GFP*). The rescue effects by the different MIG-10 isoforms on defective cell migration or excretory canal outgrowth were then quantitatively assessed *in vivo*. Cell-specific expression of isoform MIG-10A was also tested for rescuing effects on the migration of the mechanosensory neurons ALM and AVM.

PROJECT GOAL B: Preparation of Co-immunoprecipitation to test MIG-10/ABI-1 interaction in insect system

Previously the ABI-1/MIG-10 interaction was identified using a yeast two hybrid system (Gossellin and O'Toole, 2008). However, the positive result could have been caused by self-activation and thus needs to be confirmed in another system, in this case co-immunoprecipitation (Co-IP). Another goal of this Major Qualifying Project (MQP) was to initiate the preparation for confirming the ABI-1/MIG-10 interactions by Co-IP of the target proteins in insect cells using fusion tags as markers. The constructs obtained from the previous yeast two hybrid experiments were transferred into vectors of an insect expression system using the Gateway System© from Invitrogen.

Materials & Methods

TRANSFORMATION OF COMPETENT CELLS

Competent cells (Top-10 One-Shot Competent *E.coli*©) were transformed with the plasmids obtained from the BP/LR reaction, or with DNA from Qiagen minipreps. 1µL clo-nase reaction was added to 50uL competent *E. coli* cells and was incubated for 30min on ice. After heat shock for 30 seconds at 42°C, 400µL S.O.C. recovery media were added to the cells. After incubating for 1 hour at 37°C on a nutator, two different concentrations of the cells (50µL and 200uL) were plated onto LB plates containing the appropriate antibiotics (for example, LB+50µg/mL Amp plates). Bacterial plates were then incubated for 24 hours at 37°C.

After the 24-hour incubation, single colonies (approximately 5 per construct) were grown up in 5 mL of LB media containing the appropriate antibiotics (for example 5mL LB+ 50µG/mL Amp) for 24 hours in a rotator at 37°C.

ISOLATION OF PLASMID DNA

Plasmid DNA was isolated using Invitrogen's QIAprep Spin Miniprep© kit and pro-tocol. Overnight grown *E.coli* cells were pelleted at ~1400 x g for 5 min, and then resus-pended in 250uL cold Buffer P1 (with RNAase) and transferred to 1.5mL microfuge tubes. 250µL Buffer P2 was then added to each tube and mixed. Following this step 350uL Buffer N3 was added, and the tubes were inverted 4-6 times to ensure proper mixing. After being centrifuged at 13,000 RPM for 10 min, the supernatants were applied to QIAprep spin col-umns. The columns were spun at 13,000 RPM for 1 minute. After the flow-through was dis-carded, 500µL Buffer PB was added to each column, and spun for 1 minute at 13,000 RPM. The flow-through was removed, and 750µL Buffer PE (with ethanol) was applied to the col-

umn, spun at 13,000 RPM for 1 minute. After removing the flow-through, the columns were spun for an additional 1min and the flow-through was discarded. Finally, 50uL Buffer EB was applied to the center of the columns, and the columns were placed in 1.5mL microfuge tubes. The tubes sat for 1 minute, and were then centrifuged for 1 minute at 13,000 RPM. ALL eluted miniprep DNA was stored at -20°C, and DNA identity was confirmed by a restriction digest followed by electrophoresis.

GEL ELECTROPHORESIS

The DNA samples (digested or undigested) were electrophoresed in 1% agarose gel with 1X TBE (Tris- borate-EDTA) buffer. The New England BioLabs 1000bp DNA Ladder was used as a marker. The gels were run at 120 Volts for approximately 1 hour.

SEQUENCING

After restriction digests and electrophoresis, the identity of miniprep DNA samples were further confirmed by sequencing the plasmids with forward and reverse primers. Prior to sequencing, plasmids were quantitated on gels by comparing the digested bands with DNA ladder bands of similar intensity. Sequencing samples (12.0 uL per sample) were prepared to contain approximately 500 ng of purified plasmids (typically 2-4 uL of mini-prep DNA), 3-5 pmol of primers, and dH₂O. Sequencing samples were sent to the DNA Analysis Facility on Science Hill at Yale University. Typically, a sequencing sample contains 10-20ng per 200nt purified PCR product or 500ng purified plasmid

MAINTAINING STRAINS

All stock and mutant *C. elegans* strains used in the project were maintained on Nematode Growth Medium (NGM) agar plates spotted with *E.coli*. Worm strains currently in use were maintained approximately twice a week by transferring three L4 hermaphro-

dites with the correct phenotype to a new plate and stored at 20°C. Strains not currently in use were maintained approximately once a week and were kept at 15°C. Plates which had starved were chunked and allowed to go through one to two generations before being used.

A list of all maintained strains can be found in Table 1.

Table 1. *C. elegans* Strains maintained during project

Name	Strain	Source
RY0901	him-5(e1490);pgp-12::GFP	JSK
RY0902	him-5(e1490);flp-20::GFP	JSK
RY0907	mig-10;flp-20::GFP	EFR
RY0908	mig-10;pgp-12::GFP	EFR
TV6709	mig-10:FosAB	DCR
DACR2	mig-10:FosB	DCR
RY0923	mig-10;pgp-12::GFP:FosAB	SZ
RY0926	mig-10;pgp-12::GFP:FosB	SZ
RY0927	mig-10;flp-20::GFP;pgp-12::GFP:FosAB	SZ
RY0928	mig-10;flp-20::GFP;pgp-12::GFP:FosB	SZ
RY0929	mig-10;mec-4::MIG-10A;pgp-12::GFP	JSK
RY0930	mec-4::MIG-10A;pgp-12::GFP	JSK
CX7358	kyEx926	CB
RY0931	mig-10;flp-20::GFP;pgp-12::GFP;kyEx926	SZ
DACR_MIGAB	mig-10(ct41);wyls45, FosAB (2)	DCR
DACR_MIGADR	mig-10(ct41);wyls45, MIGADR	DCR
DACR_MIGBDR	mig-10(ct41);wyls45, MIGBDR	DCR
DACR_MIGB	mig-10(ct41);wyls45, FosB(2)	DCR
RY0932	mig-10;pgp-12::GFP:MIGADR	SZ
RY0933	mig-10;pgp-12::GFP:MIGBDR	SZ

Name	Strain	Source
RY0934	mig-10;flp-20::GFP;pgp-12::GFP:MIGADR	SZ
RY0935	mig-10;flp-20::GFP;pgp-12::GFP:MIGBDR	SZ

Abbreviations: **FosAB** = WRM 0613 bB08 + coel::GFP = wyEx2434. **FosAB(2)** = WRM 0613 bB08 + coel::GFP (independent injection). **FosB** = WRM 0613 bB07 + coel::GFP = olaEx2. **FosB(2)** = WRM 0613 bB07 + coel::GFP (independent injection). **MIGADR** = WRM 0613 bB08 with disrupted 1st exon mig-10a. **MIGBDR** = WRM 0613 bB08 with disrupted 1st exon mig-10b. **kyEx926** = unc-86::MIG-10A::GFP + odr-1::DsRed. **JSK**, Jessica Sullivan-Keiser; **EFR**, Elizabeth Fayalene Ryder; **DCR**, Daniel Colon-Ramos; **SZ**, Subaiou Zhang (this work); **CB**, Cori Bargmann

PREPARATION OF WORMS SLIDES FOR QUANTIFICATION

Prior to quantification, slides of growing worms were prepared. To prepare the agarose slides, 20 μ L of 1M sodium azide was added to 2 ml of heated 2% agarose. After vortexing, 1 drop of agar with azide was pipetted onto a blank slide, and another slide was immediately placed perpendicularly on top to make a pad of agarose. Worms were then transferred onto the slides in one of the two following ways: 1) L4 worms picked directly onto slides, or 2) all worms on plates transferred onto slides. In the first method, 3 μ L of M9 solution was added to the dry agarose/azide pad on the slide first. Up to 12 worms of Larval Stage 4 (L4) were picked directly from their plate(s) and immediately placed on/in the drop of M9 solution on the slide, after which a coverslip was quickly added to prevent the M9 solution from evaporating and to keep the worms in a lateral orientation. Alternatively, worms on a particular plate or a set of plates were washed off by M9 solution added directly onto the NGM plate, and pipetted into 1.5mL microfuge tube(s). After the worms were settled to the bottom of the microfuge tube(s), they were pipetted in 3 μ L of M9 solution onto the agarose slide. A coverslip was placed quickly on the top of the agarose pad.

QUANTIFICATION OF PHENOTYPES

These slides were examined under a compound microscope. Bright field was used to identify the age of the worm, as well as to determine the total length of the worm, the distance between worm vulva to worm pharynx, or the distance between pharynx to the tip of nose. Epi fluorescence was used to quantify the phenotype of interest through measurement of cells labeled by fluorescent transgenes, such as length of the excretory canal (*pgp-12::GFP*) or the position of migrations of ALM and AVM cells (*flp-20::GFP*). Quantifications were done using the IPLab software, which calculated the distances in pixels.

In the analysis of excretory cell truncation, the length of excretory cell was measured both anterior and posterior from the cell body. The distance between worm pharynx to the tip of its nose and the total length of the worm were also measured to normalize the truncation data, respectively. In the analysis of ALM and AVM migrations, distance from vulva to the final locations of both ALM cells and AVM cell were measured, as well as from vulva to worm pharynx to normalize the data.

STATISTICAL ANALYSIS

In order to determine if the differences in excretory canal truncations and neuronal cell migrations were statistically significant between different strains, all data were analyzed by univariate analysis of variance (ANOVA) followed by Post Hoc test (Tukey HSD) with SPSS statistical analysis program. The null hypothesis was that there is no difference between the different strains. When $p < 0.05$, it was assumed that the difference seen between the strains was significant; whereas if $p > 0.05$, the difference seen between strains was due to biological variation and not significant.

Results

GENETIC CROSSES

In order to test which MIG-10 isoform rescues excretory canal truncation and neuronal cell migration defects, we pursued the strategy where fosmid transgenes expressing different combinations of MIG-10 isoforms (Figure 4) were crossed into *mig-10* mutant background to create various genetic cross *C.elegans* strains (Table 2).

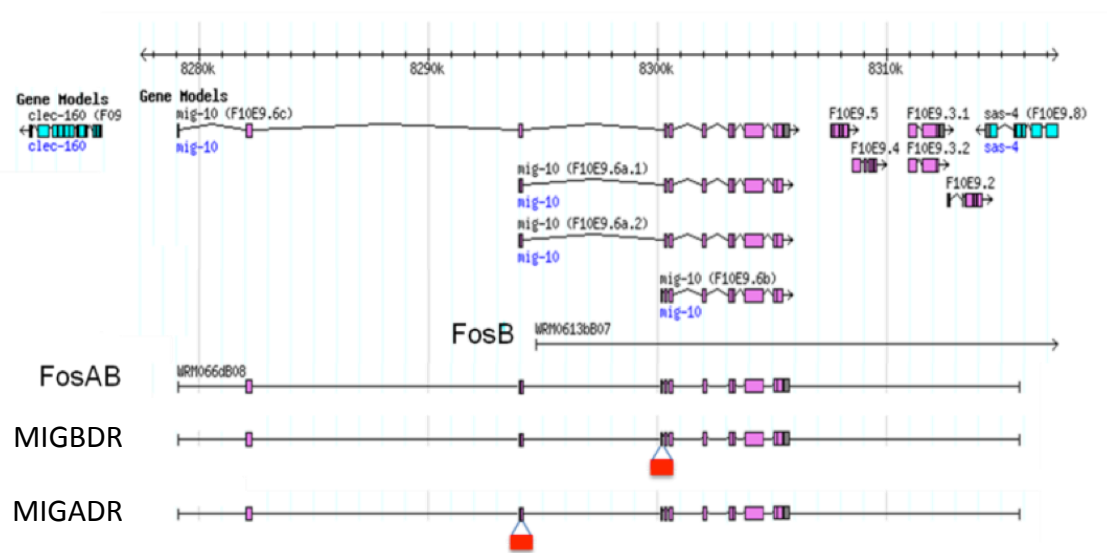


Figure 4. *mig-10* genomic constructs. (Ryder, unpublished data)

The three *mig-10* transcripts (A, B, and C) are shown at the top of the figure (the two *mig-10a* transcripts shown are virtually identical). Purple boxes represent exons. Red boxes represent mCherry marker DNA, which is inserted into the first exon of *mig-10a* or *b*, and disrupts function of the respective isoform. Coinjections were done by Daniel Colón-Ramos' lab with *coel::GFP* as cotransgenic marker. Figure modified from Wormbase (<http://www.wormbase.org/>)

Fosmids can be used to generate reporter constructs in *C. elegans*, whose genome is almost entirely covered in a readily available fosmid library (Tursun *et al.*, 2009). Fosmids expressing isoforms MIG-10 A and B together (FosAB) and B individually (FosB) were used in this project. MIG-10 A and B should be expressed in native pattern because they are in the context of complete genomic region. FosAB begins in the middle of the first exon of

mig-10c and thus should not express a functional isoform C (Figure 4). Upon injection, fosmids form large “arrays” of DNA, which are not stably integrated into chromosome. As a result, some of the transgenic progeny can lose their fosmid arrays (unrescued siblings) and exhibit *mig-10* mutant phenotype (see “FosAB sibs”, Fig.6 and Fig. 7).

These fosmid and worm strains expressing them are kindly made available to us by Dr. Daniel Colón-Ramos. The Colón-Ramos’ lab has also provided us with disruption strains, where recombineering was used on FosAB to disrupt the first exon of *mig-10b* with the mCherry marker to create MIGBDR with intact MIG-10A function and disrupted *mig-10b* transcript. A similar construct, MIGADR, was made by disrupting the first exon of *mig-10a* with mCherry (Figure 4). These strains were also crossed into *mig-10* mutant animals with excretory cell and mechanosensory neuron markers, and will be quantitatively analyzed in the future.

Table 2. *C. elegans* Strains constructed during project

Name	Strain	Created from		
RY0923	<i>mig-10</i> ;pgp-12::GFP:FosAB	RY0901	TV6709	
RY0926	<i>mig-10</i> ;pgp-12::GFP:FosB	RY0901	DACR2	
RY0927	<i>mig-10</i> ;flp-20::GFP;pgp-12::GFP:FosAB	RY0902	RY0923	
RY0928	<i>mig-10</i> ;flp-20::GFP;pgp-12::GFP:FosB	RY0902	RY0926	
RY0931	<i>mig-10</i> ;flp-20::GFP;pgp-12::GFP;kyEX926	TV6709	kyEX926	DACR2
RY0932	<i>mig-10</i> ;pgp-12::GFP:MIGADR	TV6709	MIGADR	
RY0933	<i>mig-10</i> ;pgp-12::GFP:MIGBDR	TV6709	MIGBDR	
RY0934	<i>mig-10</i> ;flp-20::GFP;pgp-12::GFP:MIGADR	DACR2	RY0932	
RY0935	<i>mig-10</i> ;flp-20::GFP;pgp-12::GFP:MIGBDR	DACR2	RY0933	

Abbreviations: **FosAB** = WRM 0613 bB08 + *coel::GFP* = wyEx2434. **FosB** = WRM 0613 bB07 + *coel::GFP* = olaEx2. **MIGADR** = WRM 0613 bB08 with disrupted 1st exon *mig-10a*. **MIGBDR** = WRM 0613 bB08 with disrupted 1st exon *mig-10b*. **kyEx926** = *unc-86::MIG-10A::GFP* + *odr-1::DsRed*.

To determine whether the migration defects are rescued by MIG-10A and MIG-10B, both the excretory canal marker *pgp-12::GFP* and the mechanosensory neuron marker *flp-20::GFP* were crossed into *mig-10(ct41)* mutant strains containing FosAB and FosB transgenes. The strategy for constructing the genetic crosses is explained in detail by the example of creating *mig-10;pgp-12::GFP:FosAB* and *mig-10;pgp-12::GFP:FosB* strains (Figure 5).

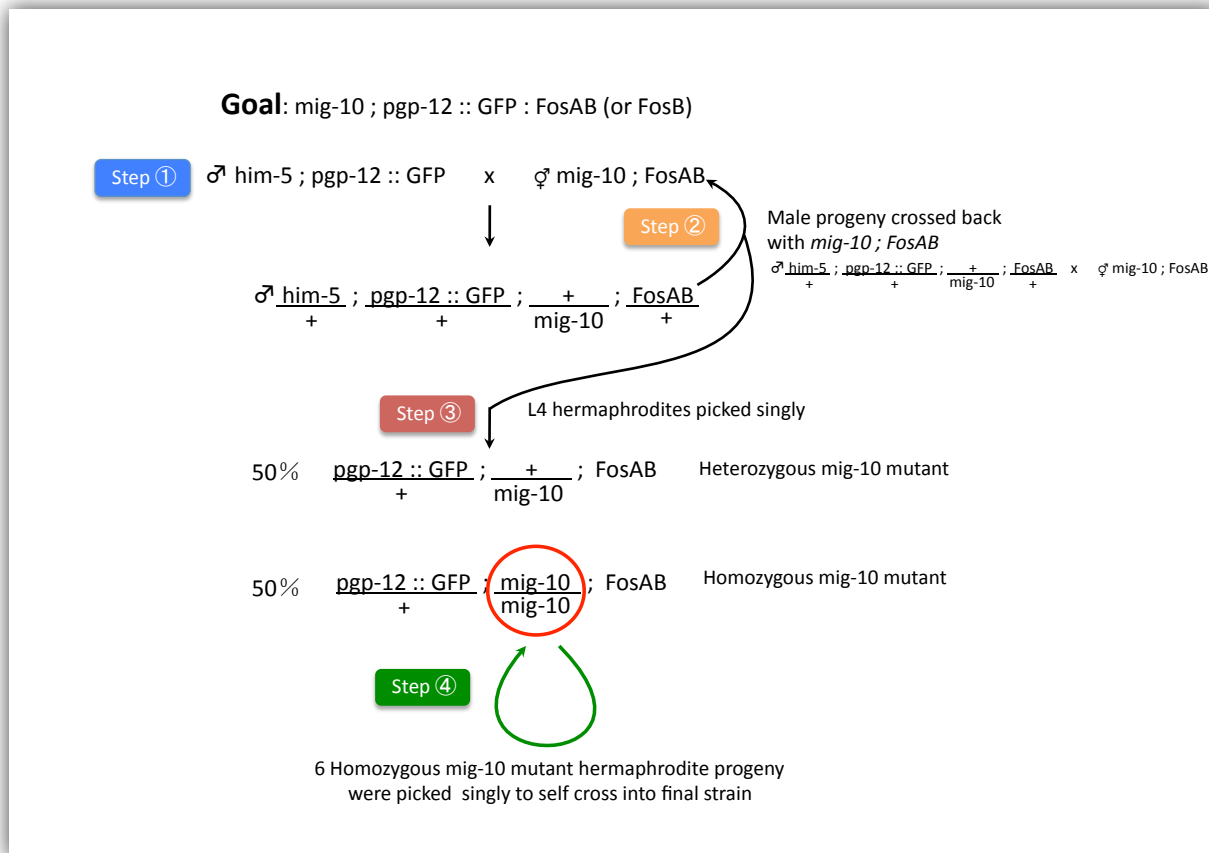


Figure 5. Strategy of constructing *mig-10;pgp-12::GFP:FosAB/mig-10;pgp-12::GFP:FosB*.

The marker strain ♂*him-5;pgp-12::GFP* contains a gene for high incidence of males (*him-5*), as well as an excretory cell marker (*pgp-12::GFP*) which labels the *C.elegans* excretory cell with GFP marker. The mutant strains (FosAB/ FosB) contain fosmid arrays expressing MIG-10 isoforms MIG-10 A and B together (FosAB) as well as B individually (FosB) with coelomocyte marker. Homozygous *mig-10* worms were selected by noting the phenotype of the progeny who have lost their fosmid arrays. In this case, the progeny of homozygous *mig-10* worm will all exhibit *mig-10* mutant phenotype, whereas some heterozygous *mig-10* progeny who have lost their fosmid arrays will still have wildtype phenotype.

FOSAB RESCUED *mig-10* MUTANT EXCRETORY CANAL TRUNCATION

The excretory canal marker *pgp-12::GFP* was crossed into *mig-10* mutant strains containing FosAB and FosB to test for rescue of excretory canal outgrowth defect. The length of the excretory canal was measured quantitatively both anterior and posterior of the excretory cell to determine whether the truncations were rescued. For posterior of the excretory cell, the data were normalized by the length of the whole animal to account for the size of the worm. Similarly, the data were normalized by the distance from posterior of the pharynx to tip of the worm's nose for anterior of excretory cell (Figure 6C).

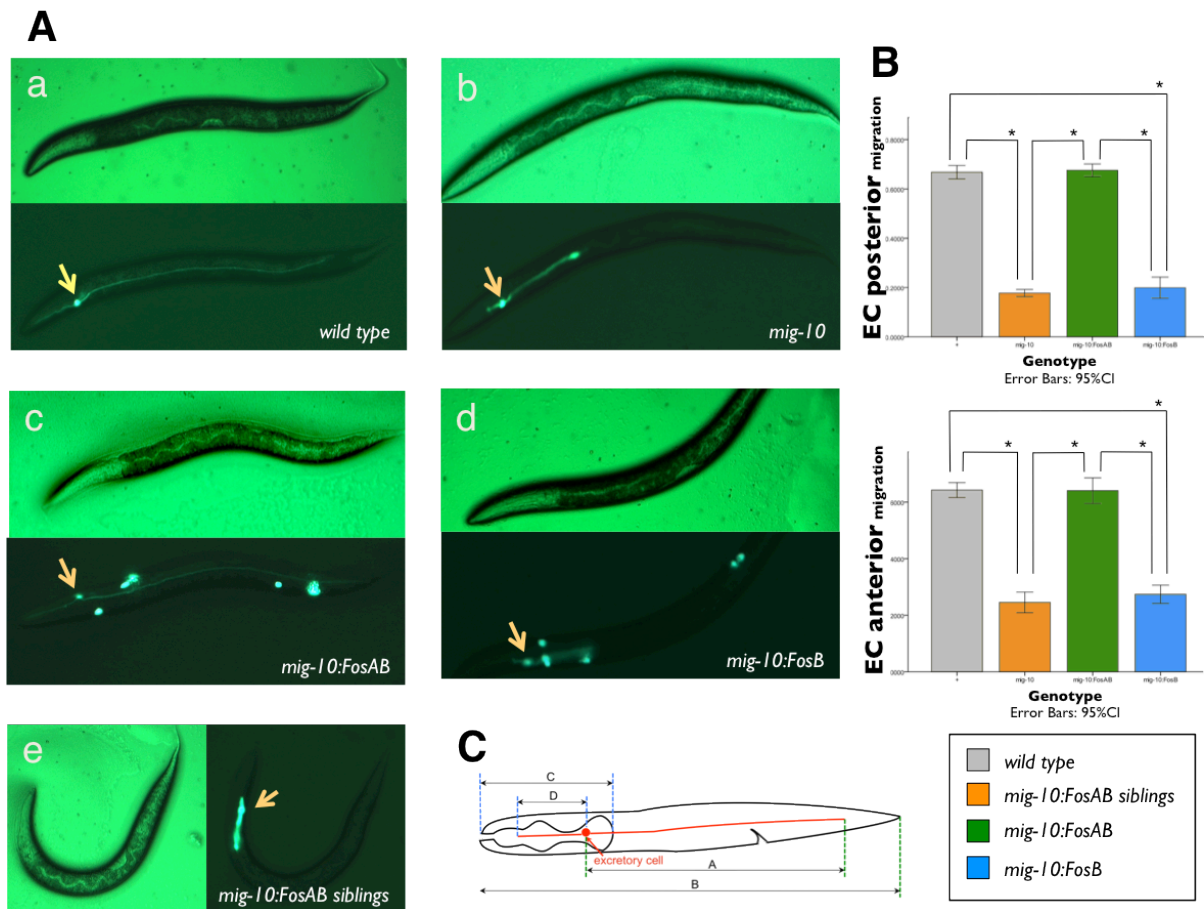


Figure 6. FosAB rescued *mig-10* mutant excretory canal outgrowth.

A) Excretory canal morphology, arrows indicate cell body. All strains have the *pgp-12::GFP* marker, expressed in the excretory cell. Bright-field and fluorescent photomicrographs, anterior to the left of worms. B) Quantitation of excretory canal outgrowth. Asterisks and brackets represent the mean differences are significant at $p < 0.05$, ANOVA followed by Tukey HSD post-hoc tests. C) Schematics of quantitation strategy. EC posterior migration = A/B , EC anterior migration = D/C .

In wild type animals, the canal reaches nearly the full length of the worm (Figure 6Aa), while in *mig-10* mutants, it is severely truncated (Figure 6Ab). Quantitative results showed that the excretory canal outgrowth in *mig-10:FosAB* animals (Figure 6Ac) were not different from wildtype animals (posterior $p=0.964$, anterior $p=1.000$), reaching nearly the full length of the worm. The truncations in *mig-10:FosAB* unrescued siblings (Figure 6Ae), which have lost their FosAB arrays and exhibit *mig-10(ct41)* mutant phenotype were not different from the *mig-10:FosB* (Figure 6Ad) animals (posterior $p=0.699$, anterior $p=0.661$). In addition, the canal outgrowth in both wildtype (*pgp-12::GFP*) and *mig-10:FosAB* animals were significantly different from both *mig-10:FosAB* unrescued siblings and *mig-10:FosB* animals (posterior and anterior $p<0.0001$). These data suggest that the defect in excretory canal migration was completely rescued by FosAB, but not by FosB (Figure 6B).

FOSAB RESCUED *mig-10* MUTANT ALM & AVM CELL MIGRATION

The mechanosensory neuron marker *flp-20::GFP* was crossed into *mig-10* mutant strains containing FosAB to test for rescue of the neuronal migration defect. Due to technical difficulties experienced with strains, FosB was not tested for rescue. The distance of the final locations of neuronal migrations (ALM1, ALM2 and AVM) to the vulva were measured quantitatively to determine whether and which migration defect were rescued. In this case, ALM1 refers to the neuron that has migrated less (ended up further from vulva) between the two ALM neurons. The data were normalized by the distance from the pharynx to vulva to account for the size of the worm (Figure 7B).

Quantitative results showed that the ALM and AVM migrations in *mig-10:Fos AB* animals (Figure 7Ac) were not different from the wildtype (Figure Aa) animals (ALM1 $p=0.064$, ALM2 $p=0.940$, AVM $p=0.586$). Both ALM and AVM neurons migrated less in

mig-10:FosAB unrescued siblings (which have lost their FosAB arrays), and were not different from *mig-10(ct41)* mutant animals (Figure 7Ab). In addition, the cell migrations in both wildtype and *mig-10:FosAB* animals were significantly different from *mig-10:FosAB* unrescued siblings and *mig-10* mutant animals ($p < 0.01$). These data indicate that the defect in both ALM and AVM cell migration were completely rescued by FosAB (Figure 7C).

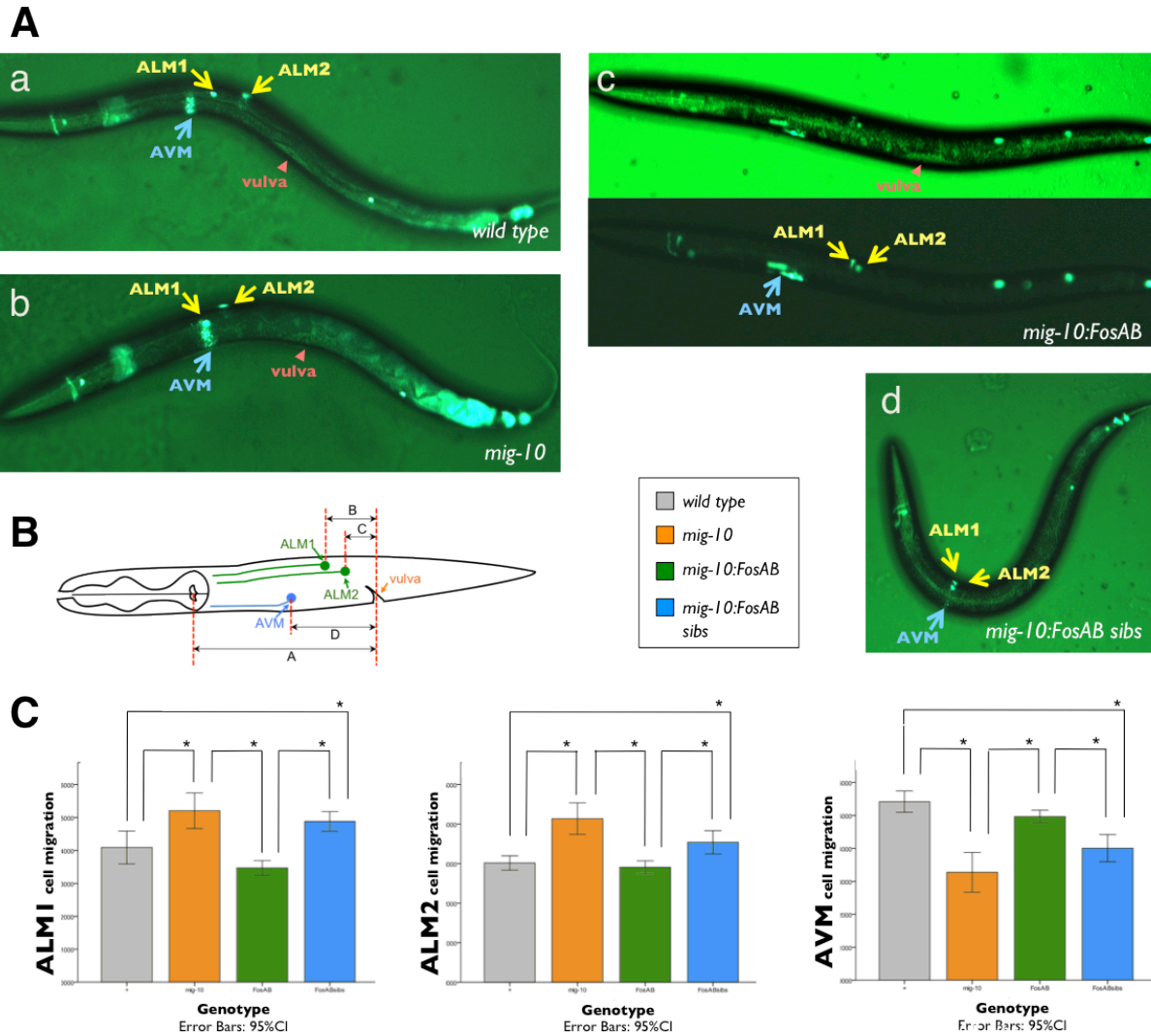


Figure 7. FosAB rescued *mig-10* mutant neuronal migration.

A) ALM and AVM morphology, arrows indicate cell body. All strains have the *flp-20::GFP* marker, expressed in the mechanosensory neurons. Fluorescent photomicrographs, anterior to the left of worms. B) Schematics of quantitation strategy. ALM1 migration = B/A , ALM2 migration = C/A , AVM migration = D/A . C) Quantitation of ALM and AVM migration. Asterisks and brackets represent the mean differences are significant at $p < 0.05$, ANOVA followed by Tukey HSD post-hoc tests.

CELL-AUTONOMOUS EXPRESSION OF MIG-10A RESCUED ALM BUT NOT AVM CELL MIGRATION

MIG-10A was over-expressed in ALM and AVM by using the *mec-4* promoter to test whether expression of the MIG-10A isoform within the cells is sufficient to rescue their migration. In this case, one control was the integrated construct without the *mig-10* mutant background. Because the construct stably expressed cDNAs for MIG-10A from cell specific promoters, there were no unrescued siblings in its progeny; thus, comparisons for rescue were made with *mig-10(ct41)*. The distance of the final locations of neuronal migrations (ALM1, ALM2 and AVM) to the vulva were measured quantitatively to determine whether and which migration defects were rescued. As before, ALM1 refers to the neuron that has migrated less (ended up further from vulva) between the two ALM neurons. The data were normalized by the distance from the pharynx to vulva to account for the size of the worm (Figure 8B).

Quantitative results showed that the ALM migrations (both ALM1 and ALM2) in *mig-10;mec-4:MIG-10A* animals (Figure 8Ad) were not different from the integrated construct control *mec-4:MIG-10A* (Figure 8Ac) animals (ALM1 $p=1.000$, ALM2 $p=0.767$). The ALM migrations of both *mig-10;mec-4:MIG-10A* and *mec-4:MIG-10A* animals (control) were different from *mig-10(ct41)* mutant (Figure 8Ab) animals ($p<0.05$). These data suggest that the cell-specific expression of MIG-10A in ALM was able to rescue the defect in ALM cell migration (Figure 8C). Interestingly, both *mig-10;mec-4:MIG-10A* and *mec-4:MIG-10A* animals (control) were different from the wild type animals (Figure 8Aa). Specifically, the overexpression of MIG-10A caused the ALMs to migrate further when comparing to wildtype animals (Figure 8C).

In contrast, the AVM migrations in *mig-10;mec-4:MIG-10A* animals were not different from *mig-10(ct41)* mutant animals ($p=0.057$), while the integrated construct control *mec-4:MIG-10A* animals were not different from the wild type animals ($p=0.655$). These data suggest that the cell-specific expression of MIG-10A in AVM was not sufficient to rescue the defect in AVM cell migration (Figure 8C).

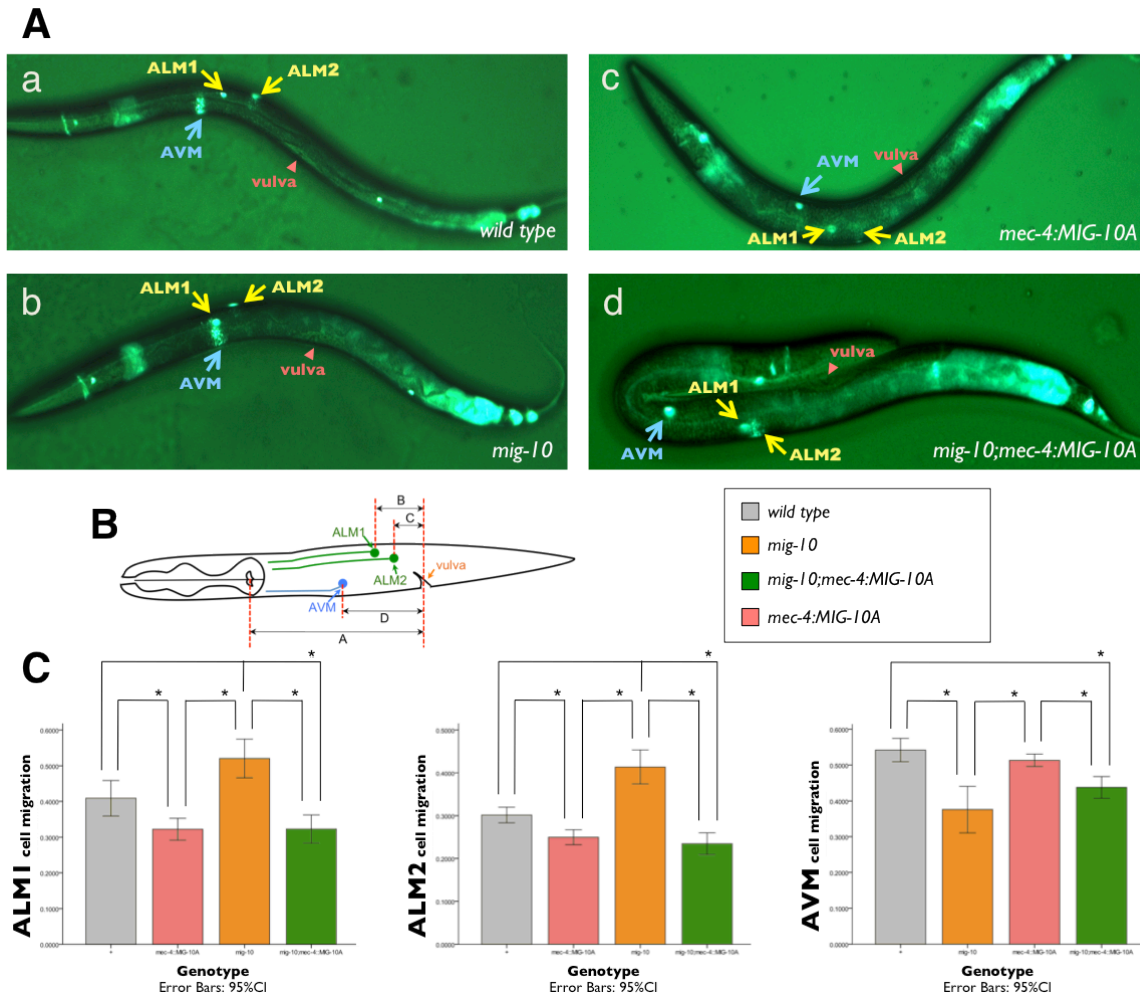


Figure 8. MIG-10A expressed cell-autonomously rescued *mig-10* mutant ALM migration but not AVM.

A) ALM and AVM morphology, arrows indicate cell body. All strains have the *flp-20::GFP* marker, expressed in the mechanosensory neurons. Fluorescent photomicrographs, anterior to the left of worms. B) Schematics of quantitation strategy. ALM1 migration = B/A , ALM2 migration = C/A , AVM migration = D/A . C) Quantitation of ALM and AVM migration. Asterisks and brackets represent the mean differences are significant at $p < 0.05$, ANOVA followed by Tukey HSD post-hoc tests. *mec-4:MIG-10A* transgene was kindly provided by C. Quinn. Strains were generated by Jessica Sullivan-Keiser.

PREPARATION OF CO-IP

In order to confirm that the previously observed interactions of ABI-1 and MIG-10 (O'Toole and Gossellin, 2008) are not due to artifacts of the yeast two hybrid system, constructs from the previous yeast two hybrid experiments will be tested in an unrelated *Drosophila* cell culture expression system. Various pairs of ABI-1 and MIG-10 constructs, including wildtype isoform and deletion constructs, will be tested for their ability to co-immunoprecipitate in this system. As part of this MQP project, several constructs obtained from the previous yeast two hybrid system were transferred into the insect expression system for the preparation of co-immunoprecipitation experiments (summarized in Table 3).

The Gateway System© by Invitrogen was used to generate the intermediate vectors leading to the creation of the appropriate expression vectors for each construct. In the Gateway© system, Att sites were used for recombining select sequences into clones via clonase (Figure 9).

Previously, the AttB-flanked genes were generated by PCR for 4 of the genes of interest: *abi-1*, *lin-53* (another interacting candidate), *mig-10b*, and *mig-10 RAPH* (containing central Ras-association and Plextrin homology domains of MIG-10). Entry vectors of *abi-1* and *mig-10b* have also been created with the BP Clonase Reaction previously (Dubuke and Grant, 2009). In this project, expression vectors of *abi-1* and *mig-10b* constructs were generated through the recombination in LR Clonase Reaction (Figure 9) between the AttL-flanked genes from the entry vectors, and pUAST GFP or His AttR-flanked lethal gene, respectively. The resulting expression vectors contain AttB-flanked gene of interest with a GFP or 6xHis tag. The AttB site was generated by recombination of the AttL and AttR sites. Following the LR Clonase Reaction, DNA was transformed into competent *E.coli* cells. Individual colonies were selected, grown up, and isolated by miniprep. Similarly, the expression vec-

tors of *lin-53* and *mig-10* RAPH were generated, although with an extra step of BP Clonase Reaction starting from the previously made PCR products (Dubuke and Grant, 2009). Gel electrophoresis analysis confirmed the expected sizes of the generated expression vectors. Correct integration of *mig-10b*, *mig-10* RAPH, and *abi-1* into the expression vectors was further confirmed by sequence analysis (data not shown).

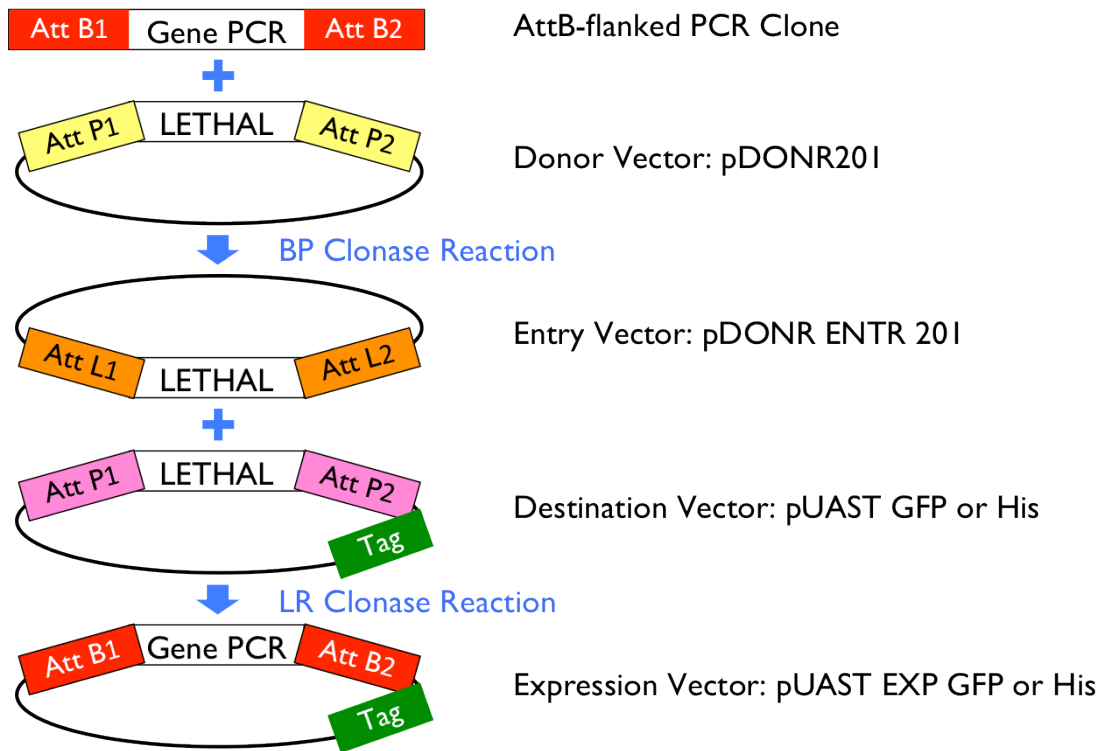


Figure 9. Schematic of expression clone generation

Through a series of cloning steps, an expression vector can be generated with a C-terminal fusion tag which can be detected by immunoblotting. Att sites are used for recombination of select sequences into clones in the sequence of: AttB+AttP -> Att L, and AttL+AttR -> AttB

Entry vectors for the *arx-3*, *mig-10a*, and *mig-10c* constructs were also generated in this project from the previously generated PCR products (Dubuke and Grant, 2009). These entry vectors were created by the BP recombination reaction between each of the AttB-flanked PCR product, and pDONR201 AttP-flanked lethal *ccdB* gene (Figure 9). DNA was

transformed into cells following the BP reaction, and individual colonies were selected, grown up, and isolated by miniprep.

Table 3. molecular constructs generated during project

PCR product	Entry vector	Expression vector	Expression vector tag	Sequencing confirmation
abi-1	D&G, 2009	this work	EGFP	✓
mig-10b	D&G, 2009	this work	6xHis	✓
mig-10a	this work			
mig-10c	this work			
mig-10 RAPH	this work	this work	6xHis	✓
lin-53	this work	this work	EGFP	
arx-3	this work			

D&G, 2009 refers to work previously done by Michelle Dubuke and Christina Grant (Dubuke & Grant, 2009)

Discussion

MIG-10 is required for axon guidance, neuronal migration, and the outgrowth of the excretory canal (Manser and Wood, 1990). To determine whether a specific MIG-10 isoform is required for complete rescue of the migration defects, fosmid genomic constructs were used to test the rescuing ability of isoforms A and B as well as B individually. Quantitative results showed that FosAB completely rescued both excretory canal truncation and ALM & AVM mechanosensory neuronal migration, suggesting that either MIG-10 isoform A or isoform B or both isoforms are sufficient to rescue *mig-10* cell and excretory canal migration defects. Although not tested directly, MIG-10 isoform C appeared to not be required for the rescue. Further experiments using disruption constructs MIGBDR and MIGADR (see Results: genetic cross for details) will address which isoform is critical for rescue of the migration defects. Experiments with these recombineered disrupted strains (made available by Dr. Daniel Colón-Ramos) will reveal if either MIG-10A or MIG-10B individually are responsible for the ability to rescue, or the expression of both isoforms is required.

To test whether cell-autonomous expression of MIG-10A is sufficient to rescue the defects in cell migration, MIG-10A cDNA was over-expressed in ALM and AVM by using the *mec-4* promoter. Quantitative results showed that this cell-specific expression of MIG-10A was able to rescue the defect in ALM cell migration, but not AVM cell migration (Figure 8Ad, 8C). The lack of rescue of the AVM cell migration is not entirely surprising, if taken into account the differences in ALM and AVM migration. The ALM and AVM cells are derived from distinct lineages via different patterns of cell divisions, where AVM progenitor (QR neuroblast) division and migration occur much earlier in the lineage (during the first larval stage) than ALM migration, which occurs during late embryogenesis (Hedgecock et al., 1987). Because *mec-4* is expressed after the ALM and AVM neurons are born (Wang &

Way, 1996), it might be too late in the cell lineage to account for the rescue of AVM. The promoter *unc-86* is expressed earlier than *mec-4* in the progenitors of these neurons (Baumeister et al., 1996), and will be tested for neuron-specific rescue to see if it can give more complete rescue. Further cell-specific expression experiments will also determine if cell autonomous expression is required for the rescue of excretory truncation. Also interesting to note is the fact that the overexpression of MIG-10A appeared to cause the ALMs to migrate further when comparing to wildtype animals (Figure 8C).

MIG-10 is shown to be required within neurons to localize actin polymerization to direct axon outgrowth (Quinn et al., 2006), but it may also act in underlying epidermal cells along which migration and excretory canal outgrowth occur. It has been speculated that MIG-10 might function in an "inside out" mechanism similar to in vertebrate T cells, transducing signals in epidermal cells so that they can respond to and influence the neurons and processes migrating over them. Because the three transcripts of *mig-10* gene differ by their initial exons and their preceding promoter sequences, it has been hypothesized that different cell types might activate different promoters to allow the expression of the appropriate MIG-10 isoform to carry out a particular migration. This hypothesis can be tested from looking at both expression patterns and rescuing ability of individual isoforms. Further experiments using cell-specific promoters driving rescuing will address whether expression in both migrating neurons and underlying epidermis is necessary for rescue. Greater understanding of the mechanisms of neuronal migration in the *C.elegans* model can be applied to more complicated vertebrate systems, and will contribute to our knowledge of human nervous system and neurological disorders.

References

- Adler, C. E., Fetter, R. D., & Bargmann, C. I. (2006). UNC-6/Netrin induces neuronal asymmetry and defines the site of axon formation. *Nature Neuroscience*, 9(4), 511-518. doi:10.1038/nn1666
- Baumeister R, Liu Y, Ruvkun G. (1996). Lineage-specific regulators couple cell lineage asymmetry to the transcription of the *Caenorhabditis elegans* POU gene *unc-86* during neurogenesis. *Genes & Development*, 10(11), 1395-1410.
- Chang, C., Adler, C. E., Krause, M., Clark, S. G., Gertler, F. B., Tessier-Lavigne, M., et al. (2006). MIG-10/lamellipodin and AGE-1/PI3K promote axon guidance and outgrowth in response to slit and netrin. *Current Biology : CB*, 16(9), 854-862. doi:10.1016/j.cub.2006.03.083
- Chilton, J. K. (2006). Molecular mechanisms of axon guidance. *Developmental Biology*, 292(1), 13-24. doi:10.1016/j.ydbio.2005.12.048
- Dickson, B. J. (2002). Molecular mechanisms of axon guidance. *Science*, 298(5600), 1959-1964. doi:10.1126/science.1072165
- Drees, F., & Gertler, F. B. (2008). Ena/VASP: Proteins at the tip of the nervous system. *Current Opinion in Neurobiology*, 18(1), 53-59. doi:DOI: 10.1016/j.conb.2008.05.007
- Dubuke, M. and Grant, C. (2009). Abi-1 Interacts with Mig-10, protein interaction in neuronal migration in *Caenorhabditis elegans*. Major Qualifying Project.
- Gabel, C. V., Antoine, F., Chuang, C. F., Samuel, A. D., & Chang, C. (2008). Distinct cellular and molecular mechanisms mediate initial axon development and adult-stage axon regeneration in *C. elegans*. *Development (Cambridge, England)*, 135(6), 1129-1136. doi:10.1242/dev.013995
- Gossellin, J. and O'Toole, S. (2008). Mig-10, an Adapter Protein, Interacts with ABI-1, a Component of Actin Polymerization Machinery. Major Qualifying Project.
- Hedgecock, E. M., Culotti, J. G., Hall, D. H., & Stern, B. D. (1987). Genetics of cell and axon migrations in *caenorhabditis elegans*. *Development (Cambridge, England)*, 100(3), 365-382.

- Innocenti, M., Zucconi, A., Disanza, A., Frittoli, E., Areces, L. B., Steffen, A., et al. (2004). Abi1 is essential for the formation and activation of a WAVE2 signalling complex. *Nature Cell Biology*, 6(4), 319-327. doi:10.1038/ncb1105
- Hobert, O., 2005. Specification of the nervous system. *WormBook*, ed. The *C. elegans* Research Community, WormBook, doi/10.1895/wormbook.1.12.1, <http://www.wormbook.org>.
- Hodgkin, J., 2005. Introduction to genetics and genomics. *WormBook*, ed. The *C. elegans* Research Community, WormBook, doi/10.1895/wormbook.1.17.1, <http://www.wormbook.org>.
- Killeen, M. T., & Sybingco, S. S. (2008). Netrin, slit and wnt receptors allow axons to choose the axis of migration. *Developmental Biology*, 323(2), 143-151. doi:DOI: 10.1016/j.ydbio.2008.08.027
- Krause, M., Leslie, J. D., Stewart, M., Lafuente, E. M., Valderrama, F., Jagannathan, R., et al. (2004). Lamellipodin, an Ena/VASP ligand, is implicated in the regulation of lamellipodial dynamics. *Developmental Cell*, 7(4), 571-583. doi:DOI: 10.1016/j.devcel.2004.07.024
- Lafuente, E. M., van Puijenbroek, A. A. F. L., Krause, M., Carman, C. V., Freeman, G. J., Berezovskaya, A., et al. (2004). RIAM, an Ena/VASP and profilin ligand, interacts with Rap1-GTP and mediates Rap1-induced adhesion. *Developmental Cell*, 7(4), 585-595. doi:DOI: 10.1016/j.devcel.2004.07.021
- Lundquist, E. A., Reddien, P. W., Hartweg, E., Horvitz, H. R., & Bargmann, C. I. (2001). Three *C. elegans* rac proteins and several alternative rac regulators control axon guidance, cell migration and apoptotic cell phagocytosis. *Development (Cambridge, England)*, 128(22), 4475-4488.
- Manser, J., & Wood, W. B. (1990). Mutations affecting embryonic cell migrations in *Caenorhabditis elegans*. *Developmental Genetics*, 11(1), 49-64. doi:10.1002/dvg.1020110107
- Manser, J., Roonprapunt, C., & Margolis, B. (1997). *C. elegans* Cell migration genemig-10 shares similarities with a family of SH2 domain proteins and acts cell nonautonomously in excretory canal development. *Developmental Biology*, 184(1), 150-164. doi:DOI: 10.1006/dbio.1997.8516

- O'Donnell, M., Chance, R. K., & Bashaw, G. J. (2009). Axon growth and guidance: Receptor regulation and signal transduction. *Annual Review of Neuroscience*, *32*, 383-412.
doi:10.1146/annurev.neuro.051508.135614
- Patel, B. N., & Van Vactor, D. L. (2002). Axon guidance: The cytoplasmic tail. *Current Opinion in Cell Biology*, *14*(2), 221-229. doi:DOI: 10.1016/S0955-0674(02)00308-3
- Proepper, C., Johannsen, S., Liebau, S., Dahl, J., Vaida, B., Bockmann, J., et al. (2007). Abelson interacting protein 1 (abi-1) is essential for dendrite morphogenesis and synapse formation. *The EMBO Journal*, *26*(5), 1397-1409. doi:10.1038/sj.emboj.7601569
- Quinn, C. C., Pfeil, D. S., Chen, E., Stovall, E. L., Harden, M. V., Gavin, M. K., et al. (2006). UNC-6/netrin and SLT-1/slit guidance cues orient axon outgrowth mediated by MIG-10/RIAM/lamellipodin. *Current Biology : CB*, *16*(9), 845-853. doi:10.1016/j.cub.2006.03.025
- Quinn, C. C., Pfeil, D. S., & Wadsworth, W. G. (2008). CED-10/Rac1 mediates axon guidance by regulating the asymmetric distribution of MIG-10/lamellipodin. *Current Biology : CB*, *18*(11), 808-813.
doi:10.1016/j.cub.2008.04.050
- Quinn, C. C., & Wadsworth, W. G. (2008). Axon guidance: Asymmetric signaling orients polarized outgrowth. *Trends in Cell Biology*, *18*(12), 597-603. doi:10.1016/j.tcb.2008.09.005
- Round, J., & Stein, E. (2007). Netrin signaling leading to directed growth cone steering. *Current Opinion in Neurobiology*, *17*(1), 15-21. doi:DOI: 10.1016/j.conb.2007.01.003
- Schmidt, K. L., Marcus-Gueret, N., Adeleye, A., Webber, J., Baillie, D., & Stringham, E. G. (2009). The cell migration molecule UNC-53/NAV2 is linked to the ARP2/3 complex by ABI-1. *Development (Cambridge, England)*, *136*(4), 563-574. doi:10.1242/dev.016816
- Takenawa, T., & Suetsugu, S. (2007). The WASP-WAVE protein network: Connecting the membrane to the cytoskeleton. *Nature Reviews.Molecular Cell Biology*, *8*(1), 37-48. doi:10.1038/nrm2069
- Tessier-Lavigne, M., & Goodman, C. S. (1996). The molecular biology of axon guidance. *Science (New York, N.Y.)*, *274*(5290), 1123-1133.

- Tursun, B., Cochella, L., Carrera, I., & Hobert, O. (2009). A toolkit and robust pipeline for the generation of fosmid-based reporter genes in *C. elegans*. *PLoS One*, 4(3), e4625. doi:10.1371/journal.pone.0004625
- Wang, L., & Way, J.C. (1996). Activation of the *mec-3* promoter in two classes of stereotyped lineages in *Caenorhabditis elegans*. *Mech Dev* 56: 165-181.
- Wither, J., Galligan, B., Hawkins, N., & Garriga, G. (2004). *Caenorhabditis elegans* WASP and Ena/VASP proteins play compensatory roles in morphogenesis and neuronal cell migration. *Genetics*, 167(3), 1165-1176. doi:10.1534/genetics.103.025676
- Yaron, A., & Zheng, B. (2007). Navigating their way to the clinic: Emerging roles for axon guidance molecules in neurological disorders and injury. *Developmental Neurobiology*, 67(9), 1216-1231. doi:10.1002/dneu.20512
- Yoshikawa, S., & Thomas, J. B. (2004). Secreted cell signaling molecules in axon guidance. *Current Opinion in Neurobiology*, 14(1), 45-50. doi:DOI: 10.1016/j.conb.2004.01.005
- Yu, T. W., & Bargmann, C. I., (2001). Dynamic regulation of axon guidance. *Nature Neuroscience*, 4(11), 1169.